J. Biochem. **135**, 43–51 (2004)
DOI: 10.1093/jb/mvh005

Multimeric Structure of the PomA/PomB Channel Complex in the Na^+-Driven Flagellar Motor of *Vibrio alginolyticus*

Tomohiro Yorimitsu*, Masaru Kojima, Toshiharu Yakushi and Michio Homma†
Division of Biological Science, Graduate School of Science, Nagoya University, Chikusa-Ku, Nagoya 464-8602

Received October 3, 2003; accepted October 30, 2003

It is known that PomA and PomB form a complex that functions as a Na^+ channel and generates the torque of the Na^+-driven flagellar motor of *Vibrio alginolyticus*. It has been suggested that PomA works as a dimer and that the PomA/PomB complex is composed of four PomA and two PomB molecules. PomA does not have any Cys residues and PomB has three Cys residues. Therefore, a mutant PomB ($PomB^{cl}$) whose three Cys residues were replaced by Ala was constructed and found to be motile as well. We carried out gel filtration analysis and examined the effect of cross-linking between the Cys residues of PomB on the formation of the PomA/PomB complex. In the presence of dithiothreitol (DTT), the elution profile of the PomA/PomB complex was shifted to a lower apparent molecular mass fraction similar to that of the complex of the wild-type PomA and $PomB^{cl}$ mutant. Next, to analyze the arrangement of PomA molecules in the complex, we introduced the mutation P172C, which has been shown to cross-link PomA molecules, into tandem PomA dimers (PomA~PomA). These mutant dimers showed a dominant-negative effect. DTT could restore the function of PomA~P172C and P172C~P172C, but not P172C~PomA. Interdimer and intradimer cross-linked products were observed; the interdimer cross-linked products could be assembled with PomB. The formation of the interdimer cross-link suggests that the channel complex of the Na^+-driven flagellar motor is composed of two units of a complex consisting of two PomA and one PomB, and that they might interact with each other *via* not only PomA but also PomB.

Key words: electrostatic interaction, energy transduction, flagellar motor, sodium type, *Vibrio*.

Abbreviations: DTT, dithiothreitol; NEM, *N*-ethylmaleimide; $PomB^{cl}$, PomB mutant with three Cys residues replaced with Ala.

Many bacteria have filamentous organelles called flagella that are used for motility. Bacterial flagella rotate by means of a motor, which is embedded in the membrane at the base of the flagellar filament. The direction of motor rotation, clockwise or counterclockwise, is reversibly regulated by chemotactic signals. The torque of the motor is generated by the electrochemical potential of specific ions across the cytoplasmic membrane (*1*, *2*). Two types of motors are known, H^+-driven (*3*, *4*) and Na^+-driven (*5*, *6*). More than 40 proteins are needed to construct the motor. Genetic and physiological studies of the H^+-driven motors of *Escherichia coli* and *Salmonella typhimurium* have identified two proteins, MotA and MotB, which have four and one transmembrane-spanning segments, respectively (*7–10*). MotA and MotB form a H^+ channel complex from their transmembrane segments (*11–13*). The MotA/MotB complex surrounds the rotor part of the motor and functions as the stator part by being attached to the peptidoglycan layer of the cell *via* a binding motif in the periplasmic domain of MotB (*14–16*). To generate the torque of the flagellar motor, the conformation of the MotA/MotB complex is thought to be changed by the H^+ flux, and this change is transmitted to FliG, which is a component of the rotor or motor/switch complex. This complex is formed by three proteins, FliG, FliM and FliN, and is required not only for torque generation, but also for flagellar assembly and for the regulation of the direction of rotation of the flagellar motor (*17–19*).

Some bacteria, such as alkaliphilic *Bacillus* and *Vibrio* species, use the electrochemical potential of Na^+ ions to generate the torque of the flagellar motor (*20*, *21*). Four proteins—PomA, PomB, MotX, and MotY—have been shown to be necessary for the rotation of the polar flagellar motor of *Vibrio* spp., *V. alginolyticus*, *V. parahaemolyticus*, and *V. cholerae*. *V. alginolyticus* and *V. parahaemolyticus* also possess H^+-driven lateral flagellar motors (*22*, *23*). PomA and PomB are orthologous to MotA and MotB (Fig. 1) and interact functionally with each other (*24*, *25*). MotX and MotY, which were first characterized as motor proteins in *V. parahaemolyticus* (*26*, *27*), are unique to the Na^+-driven polar flagellar motor of *Vibrio* spp. (*28*, *29*). Although their functions are not yet clear, a recent report showed that they co-fractionate with OmpA upon sucrose gradient centrifugation, which suggests that they are located in the outer membrane (*30*).

The Na^+-type motor has advantages over the H^+-type motor for studying the rotary mechanism in the driving force is easily manipulated by changing the Na^+ concen-

*Present address: Department of Molecular, Cellular and Developmental Biology, University of Michigan, Ann Arbor, MI 48109, USA.
†To whom correspondence should be addressed. Tel: +81-52-789-2991, Fax: +81-52-789-3001, E-mail: g44416a@cc.nagoya-u.ac.jp

tration. Furthermore, Na^+-channel blockers such as amiloride and phenamil specifically inhibit the rotation of the Na^+-type motor (*31*, *32*). Based on several lines of evidence obtained using these techniques, a complex of PomA and PomB is thought to function as the Na^+ channel. The PomA/PomB complex, solubilized by β-octylglucoside and purified and reconstituted into proteoliposomes, has the ability to conduct Na^+ ions upon the generation of a transmembrane electrical gradient created by a diffusion potential of K^+ using valinomycin (*33*). The Na^+-conducting activity in proteoliposomes reconstituted with the PomA/PomB complex is specifically blocked by phenamil and no activity is detected in proteoliposomes reconstituted with only PomA. From studies of Na^+ and H^+ hybrid motors, we could convert the *E. coli* H^+-driven motor into the Na^+-driven motor by exchanging the MotA/MotB stator with the PomA/PotB7^E stator (*34*). PotB7^E is a chimera joining the N-terminal transmembrane region of PomB to the extracellular C-terminal region of MotB. Based on its apparent molecular mass as measured by gel filtration chromatography, the isolated PomA/PomB complex retaining Na^+ uptake activity seems to be composed of four PomA and two PomB molecules (*33*). However, purified PomA proteins form a stable homodimer when expressed without PomB, which suggests that PomA may also function as a dimer within a $(PomA)_4(PomB)_2$ complex. This idea is supported by the fact that when a Cys residue is introduced into PomA, which has no native Cys residues, a cross-link is formed at the motor site (*25*). Also, a tandem PomA dimer, in which two *pomA* genes are genetically fused and produce a single polypeptide when expressed, is functional as a torque generator (*35*). The introduction of a mutation into either or both halves of the tandem PomA dimer inhibits motor function. In a recent study, Braun and Blair (*36*) showed that MotB with a Cys substitution in its sole transmembrane segment forms a specifically cross-linked dimer when expressed with MotA, suggesting that MotB also functions as a dimer in the H^+-driven flagellar motor.

Here, to obtain topological information about the PomA/PomB complex, we have carried out gel-filtration analysis of the PomA/PomB complex in the presence and absence of DTT. Furthermore, we prepared PomA tandem fusion dimer proteins containing different combinations of wild-type PomA and a Cys-substituted PomA (P172C). These experiments suggest that PomA and PomB form a multimeric structure in which four copies of PomA are assembled and surround a PomB dimer. In addition, PomA and PomB are located close to each other in the complex

EXPERIMENTAL PROCEDURES

Bacterial Strains, Plasmids, Growth Conditions, and Media—*V. alginolyticus* strains NMB190 (Rif^r, Pof$^+$, Laf$^-$, Δ*pomA*) (*37*) and NMB191 (Rif^r, Pof$^+$, Laf$^-$, Δ*pomAB*) (*38*) were used and cultured at 30°C in VC medium: 0.5% (w/v) polypeptone, 0.5% (w/v) yeast extract, 0.4% (w/v) K_2HPO_4, 3% (w/v) NaCl, 0.2% (w/v) glucose or in VPG medium: 1% (w/v) polypeptone, 0.4% (w/v) K_2HPO_4, 3% (w/v) NaCl, 0.5% (w/v) glycerol. For the swarm assay, a VPG-0.25% agar plate was used. *E. coli* strain JM109 (*recA1, endA1, gyrA96, thi*$^-$*, hsdR17, relA1, supE44,* λ$^-$*,* Δ*(lac-proAB)*; [*F', traD36, proAB, lacI*^{q}*, lacZ*Δ*M15*]) was used for DNA manipulations and cultured at 37°C in LB medium. When necessary, kanamycin was added to a final concentration of 100 μg/ml for *Vibrio* cells, or 50 μg/ml for *E. coli* cells. Plasmid pKS101, a pSU41-based plasmid, was constructed to carry *his$_6$-pomA* under *lac* promoter control (*33*). Plasmid pKS101-P172C (His_6-P172C) was constructed by inserting a 0.6-kb *Dra*I–*Eco*RI fragment of pYA301-P172C (*39*) into the corresponding site of pKS101. Plasmid pKS102 harboring *his$_6$-pomA* and *pomB* under *lac* promoter control, was constructed by inserting a 1.0-kb *Hin*dIII fragment of pKS101 into the corresponding site of pSK602 (*40*). Plasmid pKS106 encodes a tandem PomA dimer (PomA~PomA) under *lac* promoter control, and was constructed by linking two *pomA* open reading frames in frame with a 22-residue linker, MHYPYDVPDYAIEGRM-His_6, which comprises a hemagglutinin (HA)-tag and six histidines (His_6) (*35*). Figure 4A shows a schematic diagram indicating the restriction sites in the structure of PomA and PomA~PomA. Plasmids encoding mutant tandem PomA dimers were constructed by inserting fragments into the corresponding sites of pYA301-P172C as follows: pKS106 (PomA~P172C), 0.8-kb *Dra*I fragment of pKS106 (PomA~PomA); pKS106 (P172C~PomA), 1.0-kb *Hin*dIII fragment of pKS106 (PomA~PomA); and pKS106 (P172C~P172C), 0.8-kb *Dra*I fragment of pKS106 (P172C~PomA). Likewise, plasmids encoding tandem PomA dimers along with PomB were constructed by inserting fragments into the corresponding sites of pYA303 (*40*) as follows: pAAB101 (PomA~PomA/PomB), 0.8-kb *Dra*I fragment of pKS106 (PomA~PomA); pAAB101 (P172C~PomA/PomB), 0.8-kb *Dra*I fragment of pKS106 (P172C~PomA); pAAB101 (PomA~P172C/PomB), 1.0-kb *Hin*dIII fragment of pKS106 (PomA~P172C).

Gel Filtration Assay—The PomA/PomB complex was purified as previously described (*33*); except that DTT was not used. Membrane vesicles were prepared from NMB191 cells harboring pKS102 disrupted by a French press and solubilized by 2.5% β-octylglucoside. From the solubilized extracts, the PomA/PomB complex was purified using a Ni-NTA column (QIAGEN) followed by a MiniQ column (Amersham Pharmacia Biotech). The purified PomA/PomB complex was applied to a Superose 6 gel filtration column (Amersham Pharmacia Biotech) in the presence or absence of 5 mM DTT. The column was equilibrated with buffer containing DTT when the sample contained DTT. Each fraction was analyzed by SDS-PAGE followed by immunoblotting with anti-PomA or anti-PomB antibody (*41*).

Co-Elution Assay—The co-elution assay of tandem PomA dimer with PomB was carried out by Ni-NTA agarose chromatography as described previously (*33*, *35*). The Ni-NTA purified materials were analyzed by SDS-PAGE followed by immunoblotting with anti-PomA or anti-PomB antibody.

Co-Immunoprecipitation Assay—Immunoprecipitation with anti-PomB antibody was carried out essentially as described previously (*41*), except that anti-PomB antibodies were coupled to the protein A-Sepharose CL-4B beads (Amersham Pharmacia Biotech) using dimethylpimelimidate (Pierce Chemical) (*42*). Proteins bound to the resin were eluted as described previously (*43*), and

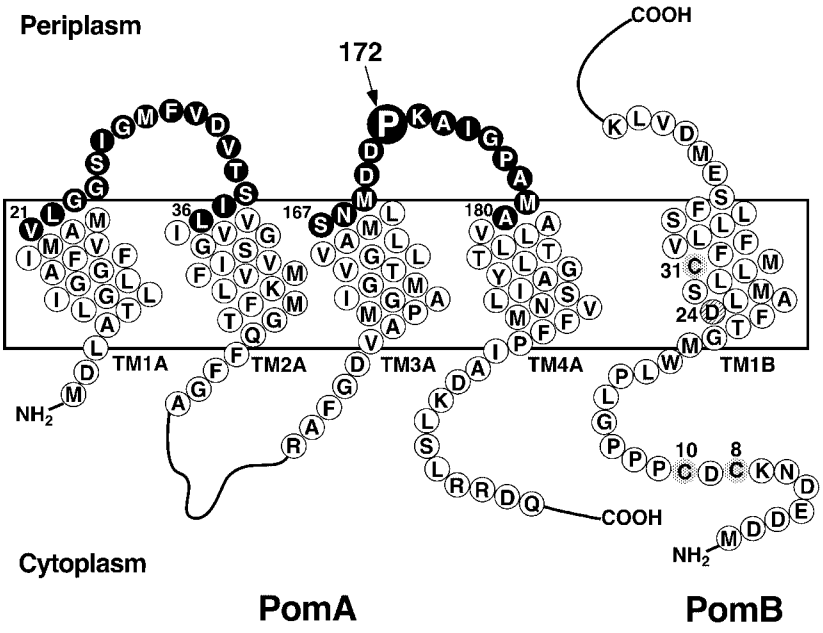

Fig. 1. **Putative membrane topology of PomA and PomB.** PomA has four transmembrane segments and no Cys residues. Amino acid residues in the putative periplasmic loops are shown as closed circles with white letters. PomB has one transmembrane segment and three Cys residues, which are shown as gray circles (C8, C10, C31). The Asp residue (D24), shown as a hatched circle, is the sole charged residue in the transmembrane segment of PomB, and is predicted to be involved in the ion pathway. Numbers indicate amino acid positions.

the eluates were analyzed by SDS-PAGE followed by immunoblotting with anti-HA (clone 12CA5) (Boehringer Mannheim) or anti-PomB antibody.

RESULTS

A Cys-Less PomB Mutant—PomA has Cys residues, whereas PomB has three, two of which, Cys8 and Cys10, are predicted to be in the cytoplasm. The other residue, Cys31, is in the transmembrane region (*24*) (Fig. 1). When SDS-PAGE was performed in the absence of a reducing reagent, wild-type PomB formed a cross-linked dimer ($PomB_2$) (Fig. 2A). Cross-linked $PomB_2$ could not be observed in the presence of reducing reagent. At the same time, the dimmer was still observed at the same level as in cells treated with NEM or expressed alone without PomA (data not shown). To determine the Cys residue responsible for the disulfide bond in PomB, mutants were constructed with Cys residues in one or more of positions 8, 10, and 31. When three Cys residues of PomB were replaced by Ala, this Cys-less PomB C8A/C10A/C31A mutant ($PomB^{cl}$) did not form the cross-linked dimer. Cells with $PomB^{cl}$ swarmed at about two-thirds the rate of those with wild-type PomB (Fig. 2B). The PomB C31A mutant and both PomB C8A/C31A and C10A/C31A double mutants formed disulfide bonds, whereas C8A/C10A mutants did not (Fig. 2A). As shown in Fig. 2B, the swarms of cells with C8A/C31A or C10A/C31A mutants were slightly poorer than the swarms of cells with the C8A/C10A mutant. The replacement of Cys31 residue may be the cause because of the decrease in the swarms of cells with the C31A single PomB mutant. Similar results were observed when Ser replaced Cys31 in the C31S mutant (data not shown). The swimming profiles were observed by microscopy and showed that the swarming sizes were roughly correlated with the swimming speeds of the mutant cells while their chemotactic behaviors were normal.

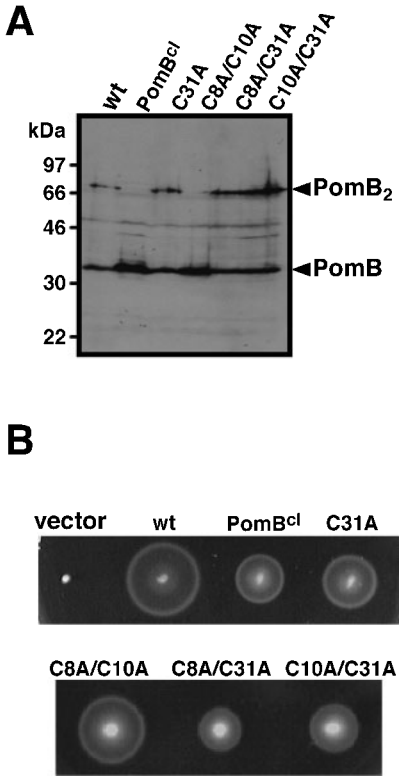

Fig. 2. **The three Cys residues of PomB are dispensable.** (A) Immunoblot using anti-PomB antibody of whole-cell lysates of *Vibrio* strain NMB191 (Δ*pomAB*) cells harboring a plasmid encoding PomA together with wild-type PomB or Ala-substituted PomB mutants. PomB mutations are shown above each lane. (B) Swarm abilities of PomB mutants with substitution of Cys residues with Ala. NMB191 (Δ*pomAB*) cells harboring a vector plasmid or a plasmid encoding PomA together with wild-type PomB or Ala-substituted PomB mutants were incubated on soft agar plates at 30°C for 4 h.

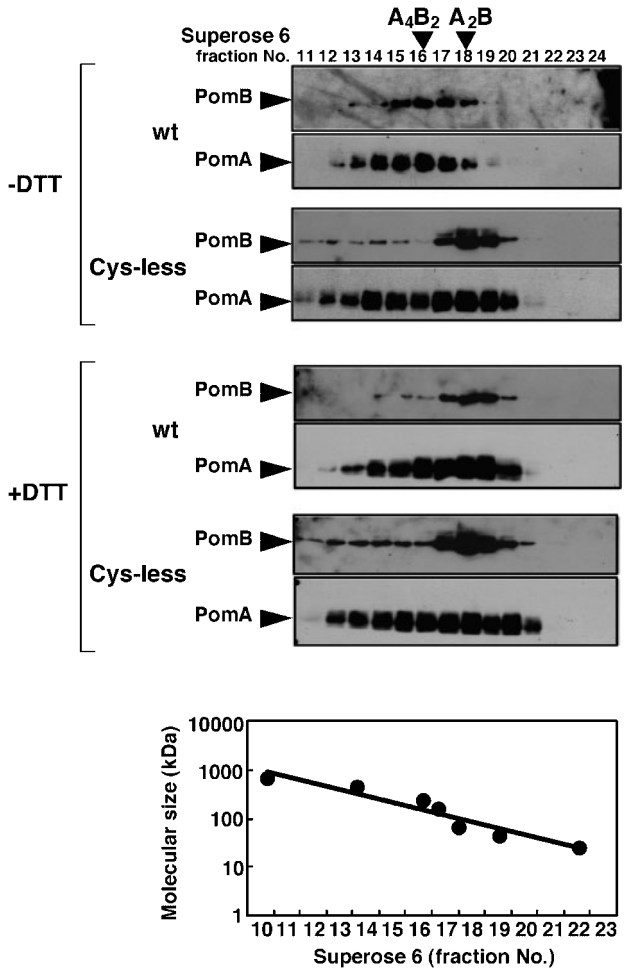

Fig. 3. **Size exclusion chromatography of the PomA/B and PomA/B^{cl} complexes.** The PomA/B and PomA/B^{cl} complexes were purified by Ni-NTA chromatography followed by MiniQ anion exchange chromatography and applied to a Superose 6 column in the absence or presence of 5 mM DTT. Anti-PomA or anti-PomB immunoblot profiles of the fractions are shown. The bottom panel shows calibration of the column with molecular standard markers: thyroglobulin (660 kDa), ferritin (440 kDa), catalase (232 kDa), aldolase (158 kDa), albumin (67 kDa), ovalbumin (43 kDa), chymotrypsinogen A (25 kDa) and RNase A (14 kDa).

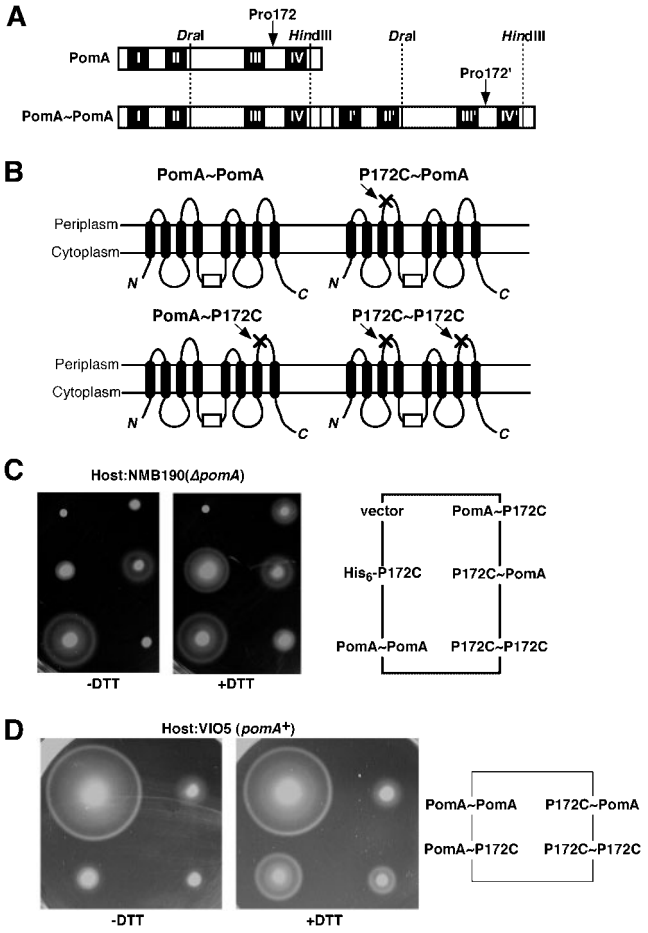

Fig. 4. **Tandem PomA dimer mutants.** (A) Restriction map of the coding regions for PomA and tandem PomA dimer. Black boxes indicate the membrane-spanning segments. (B) Schematic diagrams of various PomA~PomA tandem dimers produced as a single polypeptide. Arrows indicate the positions where amino acid substitutions were introduced. White boxes indicate the 22-residue linker. (C) Swarm abilities of tandem PomA dimer mutants. NMB190 (Δ*pomA*) cells expressing tandem PomA dimers or PomA monomer with P172C mutation were incubated on soft agar plates with or without DTT at 30°C for 6 h. (D) Dominant-negative effects of the mutant PomA dimers, using VIO5 (*pomA*$^+$) as the host.

PomB Proteins in the Isolated Torque-Generating Unit—We performed gel filtration on the purified complex in the presence or absence of DTT (Fig. 3). Gel filtration was necessary to examine whether or not the complex isolated previously as the torque-generating unit, which is believed to be a complex of $(PomA)_4(PomB)_2$ (*33*), can form the cross-link between the two PomB proteins in the unit. Based on molecular markers and the micellar size of β-octylglucoside (21 kDa), the estimated molecular mass is approximately 170–180 kDa, which correlates with the molecular mass of the $(PomA)_4(PomB)_2$ complex (180 kDa). The purified PomA/PomB complex migrated between aldolase (158 kDa) and albumin (67 kDa) in the presence of DTT. PomA and PomB eluted in later fractions than in the absence of DTT, with an estimated molecular mass of *ca.* 90 kDa, half the size of the hypothetical complex in the absence of DTT. The DTT-dependent shift in the elution of the PomA/PomB complex could be due to a reduction of cross-linking between the two PomB proteins. To investigate this possibility, we isolated the PomA/PomB^{cl} complex and analyzed it by gel filtration chromatography. PomA and PomB^{cl} co-eluted between aldolase (158 kDa) and albumin (67 kDa) even in the absence of DTT, which is at the same position as the wild-type PomA/PomB complex in the presence of DTT. We conclude that the PomB molecules are joined by one or more disulfide bonds in the purified native complex. These findings suggest that the PomB molecules are located close together in the functional complex and that the $(PomA)_4(PomB)_2$ complex seems to be assembled from two units of $(PomA)_2PomB$.

Tandem PomA Dimers and Their Effects on Motility—Previously, it was shown that tandem PomA dimers (PomA~PomA) expressed as a single polypeptide can function in the flagellar motor (*33*, *35*). When Pro172 in

the periplasmic $loop_{3-4}$ of PomA monomer is replaced by Cys, cross-linking occurs between the two PomA molecules (*25*). Native PomA contains no Cys residues. To analyze the arrangement of the PomA molecules in the complex, we substituted Cys for the Pro172 residue in either or both of the PomA subunits of the tandem PomA dimer. The three mutant tandem PomA dimers were named PomA~P172C, P172C~PomA, and P172C~P172C (Fig. 4B).

The swarming ability of Δ*pomA* cells expressing each of the Cys-substituted PomA dimers was assessed on soft agar in the absence or presence of DTT (Fig. 4C). When monomeric P172C PomA (His_6-P172C) was expressed in *Vibrio* cells, swarming was restored in the presence of DTT, a finding consistent with the previous results for the P172C PomA monomer without a His tag. Cells carrying P172C~PomA swarmed at about 60% of the size of cells carrying PomA~PomA in the absence of DTT, whose swarm was unaffected by DTT as in the case PomA~PomA. On the other hand, the swarming ability of cells producing PomA~P172C or P172C~P172C was severely inhibited in the absence of DTT. As with His_6-P172C, swarming was restored by the addition of DTT. Moreover, when cells containing PomA~P172C or P172C~P172C were placed under a dark-field microscope, swimming was found to be restored immediately following the addition of DTT (data not shown).

To investigate possible dominant-negative effects, each of the mutant tandem PomA dimers was expressed in VIO5 cells (Fig. 4D), which is wild-type for polar-flagellated motility. All three tandem PomA dimers carrying at least one P172C mutation exhibited dominant-negative effects. The P172C~P172C mutant dimer inhibited the swarming of VIO5 cells most severely (Fig. 4D, left panel). Swarming ability, except in the case of P172C~PomA, was restored in the presence of DTT (Fig. 4D, right panel). Taken together, these results suggest that tandem Cys-containing PomA dimers assemble into the torque-generating complex even when the Cys residues participate in disulfide cross-links.

Biochemical Analysis of Cys-Containing Tandem PomA Dimers—We have described the motility phenotypes of cells producing Cys-containing tandem PomA dimers. Next, we examined the proteins themselves. Membrane fractions were prepared from cells expressing the PomA monomer or tandem PomA dimer. The membrane fractions were then subjected to SDS-PAGE with or without reducing reagent followed by immunoblotting with anti-PomA antibody (Fig. 5). PomA has a molecular mass of 27 kDa. When SDS-PAGE was performed with DTT (Fig. 5, left panel), the tandem PomA dimer migrated at a position corresponding to about 50 kDa. The monomeric PomA tagged with hexameric His residues (His_6-PomA and His_6-P172C) migrated around 25 kDa. The entire tandem PomA dimers were stably expressed in the membrane, which confirmed results of previous mutagenesis studies (*35*).

When SDS-PAGE was carried out in the absence of DTT (Fig. 5, right panel), a cross-linked dimer was observed with His_6-P172C. With the tandem PomA dimers containing P172C substitutions, bands were observed with higher apparent molecular masses than the bands detected with DTT. With PomA~P172C and

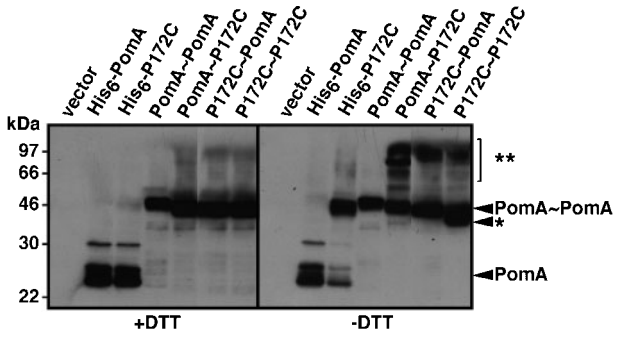

Fig. 5. **Expression of tandem PomA dimers.** Membrane vesicles (each 10 μg of protein) of NMB190 (Δ*pomA*) harboring a vector plasmid, a plasmid encoding His_6-PomA, His_6-P172C, tandem PomA dimer (PomA~PomA), or tandem PomA dimer mutants were subjected to 12% SDS-PAGE in the presence (right panel) or absence (left panel) of DTT, and immunoblotted with anti-PomA antibody. Single and double asterisks indicate putative intra- and intermolecular cross-linked products, respectively.

P172C~PomA, bands were observed around 100 kDa (double asterisks), presumably corresponding to cross-linked tandem dimers. With P172C~P172C, we also detected a band with slightly faster mobility than in the presence of DTT (asterisk), which is probably due to intramolecular cross-linking and therefore has a slightly different conformation. When membrane vesicles containing P172C~P172C were treated with $CuCl_2$, this band was enhanced (data not shown). Thus the cross-linking patterns differ among the Cys-substituted tandem PomA dimers. The cross-linking occurred not only between tandem PomA dimers, but also in the case of P172C~P172C within a tandem dimer. We infer that the P172 residues of the periplasmic $loop_{3-4}$ of each tandem dimer are close to each other. This is probably true in the case of a tetrameric complex of consisting of four molecules of normal (non-tandem) PomA.

Interaction between Tandem PomA Dimer Mutants and PomB—We investigated the effects of the cross-linking of P172C-substituted PomA dimers on the interaction with PomB. We performed a co-elution assay on a Ni-NTA column in the absence of DTT (Fig. 6A). PomB co-eluted with His-tagged PomA~PomA, P172C~PomA, and PomA~P172C. Intermolecular cross-linking also occurred with the Cys-substituted dimers. PomB did not co-elute with P172C~P172C. To investigate whether or not the formation of cross-linked P172C-substituted tandem PomA dimers affects the interaction with PomB, we performed a co-elution assay in the presence of DTT (Fig. 6B). This abolished the cross-linking of tandem dimers with PomA~P172C and P172C~PomA, but had no significant effect on the interaction with PomB. PomA~PomA also interacted with PomB under these conditions. In the presence of DTT, PomB co-eluted with P172C~P172C, although in significantly lower amounts than with other tandem dimers.

We also analyzed the interaction between tandem PomA dimers and PomB using an immunoprecipitation assay using anti-PomB antibody. Immunoprecipitates were subjected to SDS-PAGE followed by immunoblotting with anti-PomB or anti-HA antibodies because the two PomA molecules in the tandem dimer are linked

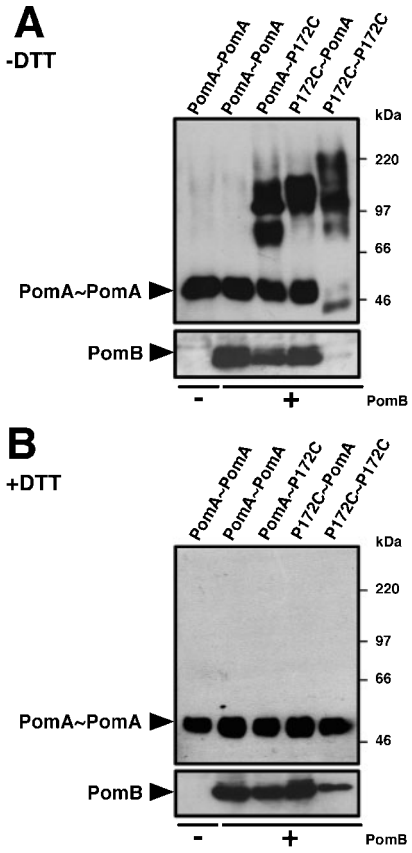

Fig. 6. **Co-elution analysis of PomB with tandem PomA dimers.** Detergent extracts from membrane vesicles of NMB191 (Δ*pomAB*) producing PomA~PomA alone, or PomB with PomA~PomA, PomA~P172C, P172C~PomA or P172C~P172C were incubated with Ni-NTA agarose resin. Eluates in the absence (A) or presence (B) of 1 mM DTT were precipitated with TCA and analyzed by SDS-PAGE in the absence of reducing reagent and immunoblotted with anti-PomB or anti-PomA antibody.

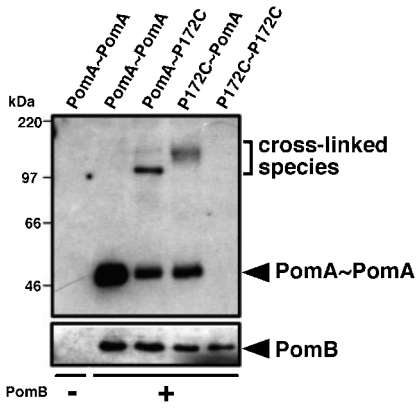

Fig. 7. **Co-immunoprecipitation of PomA tandem dimers with PomB.** Detergent extracts from membrane vesicles of NMB191 (Δ*pomAB*) expressing PomA~PomA alone, or PomB with PomA~PomA, PomA~P172C, P172C~PomA or P172C~P172C were incubated with the anti-PomB antibody immobilized to the protein A-Sepharose bead. Bound proteins were eluted, precipitated with TCA, and analyzed by SDS-PAGE in the absence of reducing reagent and immunoblotted with anti-HA or anti-PomB antibody.

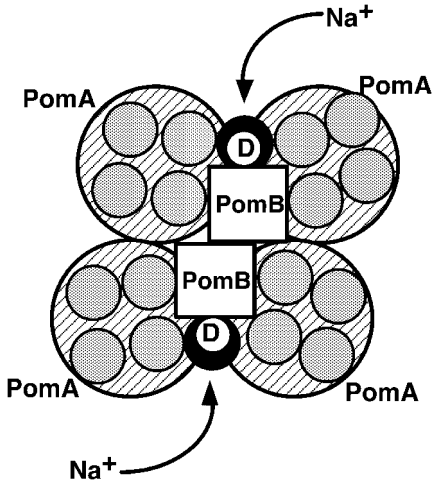

Fig. 8. **Hypothetical structural model of the PomA/B complex.** The channels are shown in the PomA/B complex, as viewed from the periplasm. In this model, the PomA/B complex has two ion-conducting channels. The Asp24 residues (circled Ds) are the only negatively charged residues in the transmembrane segment of the complex and are believed to be involved in Na^+ conductance. Note that they are not equivalently placed with respect to the two adjacent PomA molecules. The putative channel pores are indicated by black circles. The positions of the PomA and PomB transmembrane helices are shown by gray circles and open squares, respectively. The precise arrangement of either the subunits or the transmembrane helices has not yet been determined.

through 22 amino acid residues, including a hemagglutinin (HA) tag (Fig. 7). PomA~PomA, PomA~P172C, and P172C~PomA all co-precipitated with PomB. The mobilities of the cross-linked forms of PomA~P172C and P172C~PomA were different, which might have resulted from different conformations of the cross-linking of PomA~P172C and P172C~PomA. Although PomB immunoprecipitated significantly with the anti-PomB antibody, no P172C~P172C protein was detected. These results suggest that both reduced and cross-linked forms of PomA~P172C and P172C~PomA have the ability to interact physically with PomB, whereas P172C~P172C is able to do so only in the reduced form.

DISCUSSION

A previous study showed that the β-octylglucoside-solubilized PomA/PomB complex can be reconstituted into proteoliposomes and has Na^+-conducting activity (*33*). The purified Na^+-channel complex seems to be composed of four PomA and two PomB molecules with an estimated molecular mass of 175 kDa. This complex corresponds to the complex isolated in the present study in the absence of DTT. Our results indicate that the PomA/PomB complex in the presence of DTT is decreased to half its size in the absence of DTT. PomB has two Cys residues in its cytoplasmic region (Cys8 and Cys10) and one residue (Cys31) in its sole transmembrane segment (*24*). The PomA/PomB^{cl} complex composed of PomA and PomB with its three Cys residues replaced by Ala elutes in the same manner as PomA/PomB in the presence of DTT. Cells expressing PomA and PomB^{cl} are almost fully motile, which demonstrates that the PomA/PomB^{cl} complex functions properly as a torque generator and Na^+ channel

(Fig. 2). Two PomB molecules are likely to be linked to each other *via* Cys8 and/or Cys10 by disulfide cross-linking in the complex.

We previously constructed a functional tandem PomA dimer, PomA~PomA. The tandem PomA dimer has proved to be a useful tool for studying the oligomeric state of PomA. The mutation P199L makes the motor non-functional in monomeric PomA. The mutation P199L was introduced into either the C- or the N-terminal subunit of the tandem dimer and was discovered to completely inhibit torque generation (*35*). The corresponding residue in *E. coli* MotA (Pro222) has been reported to be close to Asp32 of MotB and plays a critical role in regulating a conformational change that couples H^+ conduction to motor rotation (*44*, *45*). From gel-filtration data, it was unclear whether or not and how PomA dimers within a $(PomA)_2PomB$ complex then form the $(PomA)_4(PomB)_2$ complex (Fig. 3). To examine this question, we introduced the mutation P172C into the periplasmic loops of the tandem PomA dimer (Fig. 4B). With monomeric PomA, this mutation results in cross-linking and a loss of motor function. However, this function can be recovered by reducing the cross-link with DTT. Likewise, the tandem dimers PomA~P172C and P172C~P172C regain function upon the addition of DTT, whereas P172C~PomA is functional even in the absence of DTT (Fig. 4C). Thus, it is likely that the two PomA molecules in the dimer are not equivalent in function.

The intermolecular cross-linking profiles of PomA~P172C and P172C~PomA are different (Fig. 5). The Cys residues in PomA~P172C and P172C~PomA appear to be in different environments, which possibly explains the difference in cell motility associated with these two dimers in the absence of DTT. PomA~P172C forms additional cross-linked species other than the dimer, and these could be cross-linked with unknown proteins, or be different structural forms of cross-linked PomA~P172C, consistent with the observation that PomA~P172C is less functional than P172C~PomA. With P172C~P172C, a band with a faster mobility than the reduced form was detected under non-reducing conditions (Fig. 5). Such mobility shifts could be the result of intramolecular disulfide-bond formation. This has been observed when double Cys mutations were introduced into certain loops of the tetracycline/H^+ antiporter (*46*). We suggest that the two periplasmic $loops_{3-4}$ in the P172C~P172C molecule are close to each other; however, the alignment of the transmembrane segments has not been clarified. Three of the tandem PomA dimers we constructed showed dominant-negative effects implying that the cross-linked forms can be inserted into the motor and prevent its function. Although reduction of the cross-link by DTT restored the interaction with PomB and swarming ability, the cross-linked form of P172C~P172C could not bind PomB (Figs. 6 and 7). These results seem to be inconsistent with the idea that PomA is fixed in the motor by forming a complex with PomB, which is attached to the peptidoglycan layer (*10*, *15*, *16*, *24*). Tandem dimers with P199L mutations also could not bind PomB, yet exhibited negative dominance (*34*). They might be interacting with MotX or MotY, whose functions are not known but are essential for the rotation of the Na^+-driven motor and seem to be located in the outer membrane (*30*).

Based on the present and previous results, we propose a hypothetical structural model in which the $(PomA)_4(PomB)_2$ complex is formed from two $(PomA)_2PomB$ complexes with the two PomB molecules facing each other. The previous study showed that when expressed alone without PomB, PomA does not form a homotetramer but a stable homodimer (*41*). The association of PomB with PomA~P172C and P172C~PomA does not seem to be affected by whether or not these tandem dimers become cross-linked. In fact, pre-cross-linked tandem dimers can subsequently interact with PomB. Moreover, the $(PomA)_2PomB$ complex seems to be stable under certain conditions where reducing reagents exist and the Cys residues of PomB are replaced with Ala. From these results, we speculate that the PomA dimer and the PomB monomer are pre-assembled into the $(PomA)_2PomB$ complex and then associate with each other to form the $(PomA)_4(PomB)_2$ complex, which involves both PomA and PomB interactions. Another possibility is that PomB is first dimerized and then two copies of the PomA dimer are assembled with $(PomB)_2$. Whether or not the process of assembly *in vivo* is obligatory is uncertain and further analysis is needed for clarification.

Asp24 in PomB is believed to bind Na^+ and to be located at the interface between PomA and PomB. We propose that it forms a Na^+ channel with both subunits of the PomA homodimer and that the PomA/B complex has two Na^+-conducting pores. The idea of two-channel complexes in the flagellar motor is supported by studies using the Na^+-channel blocker phenamil, which specifically impairs motor function, presumably by blocking the Na^+ ion binding site (*31*, *47*). Mutations resulting in phenamil resistance have been isolated for both PomA and PomB (*40*, *48*), and the mutation D148Y in PomA has been characterized in some detail. Phenamil resistance resulted when this mutation was introduced into either the N-terminal or the C-terminal subunit of the tandem PomA dimer. The resistance was equivalent to the resistance that results from the introduction of mutations into both subunits (*35*). This result suggests that both subunits in PomA dimer synergistically form the binding site for phenamil. Furthermore, by implication, both subunits of the PomA dimer are necessary along with PomB for Na^+ conductance.

In the H^+-driven flagellar motor, Trp-scanning was performed against the transmembrane helices of MotA and MotB. Whether or not substitutions with Trp residues could be tolerated was determined by examining the interfaces directed toward the lipid (*49*, *50*). These studies proposed the topological arrangement of the helices in the MotA/MotB complex. A single helix of MotB is tilted relative to the helices of MotA and the cytoplasmic end of the MotB helix is embedded in the complex. This structural model was presented based on the assumption that the force-generating unit is a 1 : 1 complex of MotA and MotB and that the five transmembrane helices comprise an ion channel. In *E. coli*, Braun and Blair (*36*) performed a systematic Cys-substitution against a single transmembrane segment of MotB, which is the PomB ortholog of the H^+-driven flagellar motor of *E. coli*. They found the periodical formation of cross-links on one face of the α-helix with or without the co-expression of MotA. Therefore, it was suggested that the two copies of MotB

form a dimer in the MotA/MotB complex and the two Asp residues are displayed on separate faces. Asp24 in PomB is the only negatively charged residue in the transmembrane segments of the PomA/PomB complex. It is highly conserved among the PomB (MotB) orthologs of various species of H^+- and Na^+-driven flagellar motors and is thought to be directly involved in ion conduction. Previous studies have suggested that Asp32 in MotB of *E. coli*, which corresponds to Asp24 of PomB of *V. alginolyticus*, faces MotA to form the H^+ channel (*44*, *49*, *50*). The topological model was revised based on the stoichiometry of the force-generating unit (4:2 complex of MotA and MotB) (*51*). TM3 and TM4 of MotA are arranged in an inner layer around the TM of MotB. TM1 and TM2 of MotA are placed on the outside. This is consistent with our data that two periplasmic $loops_{3-4}$ in the A subunit molecule are close to each other. However, the topological arrangement of the transmembrane helices has yet to clarify either the packing profile of the transmembrane helices. To understand the topology of the transmembrane helices with the torque-generating unit is important to reveal the energy-coupling mechanism of the flagellar motor.

This work was supported in part by grants-in-aid for scientific research from the Ministry of Education, Science and Culture of Japan and the Japan Science and Technology Corporation (to M.H. and to T.Y.), and from the Japan Society for the Promotion of Science (to T.Y.). We thank R.M. Macnab for critically reading the manuscript and K. Sato for helpful suggestions and discussion. We dedicate this article to Robert M. Macnab, Professor of Yale University in Department of Molecular Biophysics and Biochemistry. He passed away on September 7, 2003 at the age of 63. He was a kind, gentle, fair, and unforgettable person.

REFERENCES

1. Macnab, R. (1996) *Flagella and Motility in Escherichia coli and Salmonella* (Neidhardt, F.C., chief-ed.) pp.123–145, American Society for Microbiology, Washington, D.C.
2. Blair, D.F. (1995) How bacteria sense and swim. *Annu. Rev. Microbiol.* **49**, 489–522
3. Manson, M.D., Tedesco, P., Berg, H.C., Harold, F.M., and van der Drift, C. (1977) A proton motive force drives bacterial flagella. *Proc. Natl Acad. Sci. USA* **74**, 3060–3064
4. Matsuura, S., Shioi, J., and Imae, Y. (1977) Motility in *Bacillus* subtilis driven by an artificial proton motive force. *FEBS Lett.* **82**, 187–190
5. Hirota, N., Kitada, M., and Imae, Y. (1981) Flagellar motors of alkalophilic *Bacillus* are powered by an electrochemical potential gradient of Na^+. *FEBS Lett.* **132**, 278–280
6. Imae, Y., Matsukura, H., and Kobayasi, S. (1986) Sodium-driven flagellar motors of alkalophilic *Bacillus*. *Methods Enzymol.* **125**, 582–592
7. Dean, G.D., Macnab, R.M., Stader, J., Matsumura, P., and Burks, C. (1984) Gene sequence and predicted amino acid sequence of the *motA* protein, a membrane-associated protein required for flagellar rotation in *Escherichia coli*. *J. Bacteriol.* **159**, 991–999
8. Zhou, J.D., Fazzio, R.T., and Blair, D.F. (1995) Membrane topology of the MotA protein of *Escherichia coli*. *J. Mol. Biol.* **251**, 237–242
9. Stader, J., Matsumura, P., Vacante, D., Dean, G.E., and Macnab, R.M. (1986) Nucleotide sequence of the *Escherichia coli* MotB gene and site-limited incorporation of its product into the cytoplasmic membrane. *J. Bacteriol.* **166**, 244–252
10. Chun, S.Y. and Parkinson, J.S. (1988) Bacterial motility: membrane topology of the *Escherichia coli* MotB protein. *Science* **239**, 276–278
11. Blair, D.F. and Berg, H.C. (1990) The MotA protein of *E. coli* is a proton-conducting component of the flagellar motor. *Cell* **60**, 439–449
12. Stolz, B. and Berg, H.C. (1991) Evidence for interactions between MotA and MotB, torque-generating elements of the flagellar motor of *Escherichia coli*. *J. Bacteriol.* **173**, 7033–7037
13. Tang, H., Braun, T.F., and Blair, D.F. (1996) Motility protein complexes in the bacterial flagellar motor. *J. Mol. Biol.* **261**, 209–221
14. Khan, S., Dapice, M., and Reese, T.S. (1988) Effects of *mot* gene expression on the structure of the flagellar motor. *J. Mol. Biol.* **202**, 575–584
15. De Mot, R. and Vanderleyden, J. (1994) The C-terminal sequence conservation between OmpA-related outer membrane proteins and MotB suggests a common function in both gram-positive and gram-negative bacteria, possibly in the interaction of these domains with peptidoglycan. *Mol. Microbiol.* **12**, 333–334
16. Koebnik, R. (1995) Proposal for a peptidoglycan-associating alpha-helical motif in the C-terminal regions of some bacterial cell-surface proteins. *Mol. Microbiol.* **16**, 1269–1270
17. Sockett, H., Yamaguchi, S., Kihara, M., Irikura, V., and Macnab, R.M. (1992) Molecular analysis of the flagellar switch protein FliM of *Salmonella typhimurium*. *J. Bacteriol.* **174**, 793–806
18. Irikura, V.M., Kihara, M., Yamaguchi, S., Sockett, H., and Macnab, R.M. (1993) *Salmonella typhimurium fliG* and *fliN* mutations causing defects in assembly, rotation, and switching of the flagellar motor. *J. Bacteriol.* **175**, 802–810
19. Lloyd, S.A., Tang, H., Wang, X., Billings, S., and Blair, D.F. (1996) Torque generation in the flagellar motor of *Escherichia coli*: Evidence of a direct role for FliG but not for FliM or FliN. *J. Bacteriol.* **178**, 223–231
20. Yorimitsu, T. and Homma, M. (2001) Na^+-driven flagellar motor of *Vibrio*. *Biochim. Biophys. Acta* **1505**, 82–93
21. McCarter, L.L. (2001) Polar flagellar motility of the *Vibrionaceae*. *Microbiol. Rev.* **65**, 445–462
22. Atsumi, T., McCarter, L., and Imae, Y. (1992) Polar and lateral flagellar motors of marine *Vibrio* are driven by different ion-motive forces. *Nature* **355**, 182–184
23. Kawagishi, I., Maekawa, Y., Atsumi, T., Homma, M., and Imae, Y. (1995) Isolation of the polar and lateral flagellum-defective mutants in *Vibrio alginolyticus* and identification of their flagellar driving energy sources. *J. Bacteriol.* **177**, 5158–5160
24. Asai, Y., Kojima, S., Kato, H., Nishioka, N., Kawagishi, I., and Homma, M. (1997) Putative channel components for the fast-rotating sodium-driven flagellar motor of a marine bacterium. *J. Bacteriol.* **179**, 5104–5110
25. Yorimitsu, T., Sato, K., Asai, Y., and Homma, M. (2000) Intermolecular cross-linking between the periplasmic $loop_{3-4}$ regions of PomA, a component of the Na^+-driven flagellar motor of *Vibrio alginolyticus*. *J. Biol. Chem.* **275**, 31387–31391
26. McCarter, L.L. (1994) MotY, a component of the sodium-type flagellar motor. *J. Bacteriol.* **176**, 4219–4225
27. McCarter, L.L. (1994) MotX, the channel component of the sodium-type flagellar motor. *J. Bacteriol.* **176**, 5988–5998
28. Gosink, K.K. and Häse, C.C. (2000) Requirements for conversion of the Na^+-driven flagellar motor of *Vibrio cholerae* to the H^+-driven motor of *Escherichia coli*. *J. Bacteriol.* **182**, 4234–4240
29. Okabe, M., Yakushi, T., Asai, Y., and Homma, M. (2001) Cloning and characterization of *motX*, a *Vibrio alginolyticus* sodium-driven flagellar motor gene. *J. Biochem.* **130**, 879–884
30. Okabe, M., Yakushi, T., Kojima, M., and Homma, M. (2002) MotX and MotY, specific components of the sodium-driven flagellar motor, colocalize to the outer membrane in *Vibrio alginolyticus*. *Mol. Microbiol.* **46**, 125–134

31. Sugiyama, S., Cragoe, E.J., Jr., and Imae, Y. (1988) Amiloride, a specific inhibitor for the Na^+-driven flagellar motors of alkalophilic *Bacillus*. *J. Biol. Chem.* **263**, 8215–8219
32. Atsumi, T., Sugiyama, S., Cragoe, E.J., Jr., and Imae, Y. (1990) Specific inhibition of the Na^+-driven flagellar motors of alkalophilic *Bacillus* strains by the amiloride analog phenamil. *J. Bacteriol.* **172**, 1634–1639
33. Sato, K. and Homma, M. (2000) Functional reconstitution of the Na^+-driven polar flagellar motor component of *Vibrio alginolyticus*. *J. Biol. Chem.* **275**, 5718–5722
34. Asai, Y., Kawagishi, I., Sockett, E., and Homma, M. (1999) Hybrid motor with the H^+-and Na^+-driven components can rotate *Vibrio* polar flagella by using sodium ions. *J. Bacteriol.* **181**, 6322–6338
35. Sato, K. and Homma, M. (2000) Multimeric structure of PomA, the Na^+-driven polar flagellar motor component of *Vibrio alginolyticus*. *J. Biol. Chem.* **275**, 20223–20228
36. Braun, T.F. and Blair, D.F. (2001) Targeted disulfide cross-linking of the MotB protein of *Escherichia coli*: evidence for two H^+ channels in the stator complex. *Biochemistry* **40**, 13051–13059
37. Asai, Y., Kawagishi, I., Sockett, E., and Homma, M. (1999) Hybrid motor with the H^+-and Na^+-driven components can rotate *Vibrio* polar flagella by using sodium ions. *J. Bacteriol.* **181**, 6322–6338
38. Asai, Y., Sockett, R.E., Kawagishi, I., and Homma, M. (2000) Coupling ion specificity of chimeras between H^+- and Na^+-driven motor proteins, MotB and PomB, in *Vibrio* polar flagella. *EMBO J.* **19**, 3639–3648
39. Asai, Y., Shoji, T., Kawagishi, I., and Homma, M. (2000) Cystein-scanning mutagenesis of the periplasmic loop regions of PomA, a putative channel component of the sodium-driven flagellar motor in *Vibrio alginolyticus*. *J. Bacteriol.* **182**, 1001–1007
40. Kojima, S., Asai, Y., Atsumi, T., Kawagishi, I., and Homma, M. (1999) Na^+-driven flagellar motor resistant to phenamil, an amiloride analog, caused by mutations of putative channel components. *J. Mol. Biol.* **285**, 1537–1547
41. Yorimitsu, T., Sato, K., Asai, Y., Kawagishi, I., and Homma, M. (1999) Functional interaction between PomA and PomB, the Na^+-driven flagellar motor components of *Vibrio alginolyticus*. *J. Bacteriol.* **181**, 5103–5106
42. Ungermann, C., Nichols, B.J., Pelham, H.R., and Wickner, W. (1998) A vacuolar v-t-SNARE complex, the predominant form *in vivo* and on isolated vacuoles, is disassembled and activated for docking and fusion. *J. Cell Biol.* **140**, 61–69
43. Kihara, A., Noda, T., Ishihara, N., and Ohsumi, Y. (2001) Two distinct Vps34 phosphatidylinositol 3-kinase complexes function in autophagy and carboxypeptidase Y sorting in *Saccharomyces cerevisiae*. *J. Cell Biol.* **152**, 519–530
44. Kojima, S. and Blair, D.F. (2001) Conformational change in the stator of the bacterial flagellar motor. *Biochemistry* **40**, 13041–13050
45. Braun, T.F., Poulson, S., Gully, J.B., Empey, J.C., Van, W.S., Putnam, A., and Blair, D.F. (1999) Function of proline residues of MotA in torque generation by the flagellar motor of *Escherichia coli*. *J. Bacteriol.* **181**, 3542–3551
46. Kubo, Y., Konishi, S., Kawabe, T., Nada, S., and Yamaguchi, A. (2000) Proximity of periplasmic loops in the metal-Tetracycline/H^+ antiporter of *Escherichia coli* observed on site-directed chemical cross-linking. *J. Biol. Chem.* **275**, 5270–5274
47. Kojima, S., Atsumi, T., Muramoto, K., Kudo, S., Kawagishi, I., and Homma, M. (1997) *Vibrio alginolyticus* mutants resistant to phenamil, a specific inhibitor of the sodium-driven flagellar motor. *J. Mol. Biol.* **265**, 310–318
48. Boles, B.R. and McCarter, L.L. (2000) Insertional inactivation of genes encoding components of the sodium-type flagellar motor and switch of *Vibrio parahaemolyticus*. *J. Bacteriol.* **182**, 1035–1045
49. Sharp, L.L., Zhou, J.D., and Blair, D.F. (1995) Features of MotA proton channel structure revealed by tryptophan-scanning mutagenesis. *Proc. Natl Acad. Sci. USA* **92**, 7946–7950
50. Sharp, L.L., Zhou, J.D., and Blair, D.F. (1995) Tryptophan-scanning mutagenesis of MotB, an integral membrane protein essential for flagellar rotation in *Escherichia coli*. *Biochemistry* **34**, 9166–9171
51. Blair, D.F. (2003) Flagellar movement driven by proton translocation. *FEBS Lett.* **545**, 86–95